The importance of turbulence macroscale in determining the drag coefficient of spheres

R. S. Neve*

Turbulence macroscale, from evidence provided, is at least as important as its intensity in determining the drag coefficient of spheres, particularly when macroscale and sphere diameter are comparable. Particular combinations of scale, intensity and Reynolds number can produce sudden and repeatable marked changes in flow conditions which are as important as the well known change in boundary layer conditions at critical Reynolds number. More detailed analysis suggests that other researchers' results appear sometimes to be mutually incompatible simply because they were dealing with different areas of the complicated relationship between drag coefficient, Reynolds number, turbulence intensity and macroscale.

Keywords: *sphere drag, turbulence intensity, macroscale*

Much of the published data for the drag coefficient of spheres has related to either laminar flows or flows having a relative turbulence intensity of less than a few percent. Most engineering and industrial applications, however, involve flows of considerable turbulence and in many cases designers must have resorted to a process bordering upon guesswork to obtain a value of drag coefficient C_D for use in their analyses.

The author and his associates[1-3] have published results obtained from positioning spheres on jet centrelines where the relative turbulence intensity I, defined as the rms value of the streamwise fluctuating velocity component divided by the local time mean velocity, can reach values as high as 23%. Similar values of I can also be encountered in turbulent two-phase pipe flows, wherein the settling time of any conveyed spherical solids and the axial pressure gradient in the pipe are both functions of C_D. Suspended drying processes, hydrocyclones, aerosol dispersion and airborne particles in the atmosphere are also cases where drag coefficient estimation could be difficult because of the high turbulence levels involved.

The effect of increasing the value of I is always to lower the Reynolds number Re at which C_D for a sphere drops rapidly from about 0.5 to 0.1, following transition in the sphere's boundary layer, causing an associated narrower wake. Dryden[4] defined this critical Reynolds number as the value at which C_D attains 0.3 during the drop. His value of I did not exceed a few percent because he feared loss of homogeneity if he approached too closely his turbulence generating grids. However, the results of the present author[3] extrapolate closely to Dryden's, even though the jet turbulence was not homogeneous.

Other high turbulence results were obtained by Torobin and Gauvin[5] by accelerating spherical particles along a pipe flow, calculating the value of C_D from measured acceleration rates and the known masses and sizes of particles. Some of their results are summarized in Fig 1 and it can be seen that at very high values of turbulence intensity, critical values of Re have been obtained which are between two and three orders of magnitude lower than for the standard curve given by Achenbach[6]. Subsequent results given by Clamen and Gauvin[7] extend previous figures to higher Reynolds numbers and show that a peak is obtained in the C_D curve at a Reynolds number dependent on turbulence intensity.

Such astonishingly low values of critical Reynolds number and large deviations in C_D from the standard curve were attributed to the fundamental difference between suspending spheres in a wind tunnel and allowing them free movement along a pipe flow, they being then subject to lateral as well as axial movement. This may well be so but if some appropriate results from the present author's work[3] are then superimposed, it can be seen that they tend towards the highest Reynolds number results given by Clamen and Gauvin[7]. One can now envisage the possibility of, for example, a drag coefficient curve for $I = 15\%$ extending from very low to very high Reynolds numbers and having two critical values, at just over 10^3 and at about 30×10^3, with a reversion to a high C_D value in between. This suggests that some other property, for example, turbulence macroscale, is having an effect since the curve just described has the same value of I everywhere.

Torobin, Clamen and Gauvin discount the possibility that scale has any importance here but clearly it would be valuable to test spheres in the appropriate Reynolds number range of a few thousand to a few tens of thousands, under conditions where turbulence scale and intensity are known with reasonable accuracy so that an attempt can be made to assess the importance of scale in determining drag coefficient. This was therefore the purpose of the work reported here.

* Department of Mechanical Engineering, The City University, London EC1V 0HB, UK
Also: Thermo-Fluids Engineering Research Centre
Received 11 May 1985 and accepted for publication in final form on 19 September 1985

Experimental arrangements

Turbulent airflows for these tests were produced by an open section wind tunnel having a contraction ratio of 8:1 and a working section measuring 405 x 240mm (Fig 2). Air speeds up to about 47 m/s were possible and previous testing had shown that airflow in the exit plane was of acceptably uniform velocity and had a turbulence intensity less than about 0.4%. Downstream turbulence was produced using one of three grids, placed at the exit plane. These were of the rectangular slat type, characterized by the slat width b and distance M between slat centrelines ('mesh'). Grid A had $b=25$ mm, $M=90$ mm, grid B 6 and 20 mm and grid C 2 and 14 mm respectively.

Two spheres were used: one of 115 mm diameter, used in previous testing; the other was a high quality table tennis ball with $d=37.7$ mm. The former was polished and mounted on a mild steel sting of diameter 8 mm ($=d/14.4$) and length 105 mm. The latter's surface was tested using a Talysurf and found to have an equivalent sand roughness k/d less than 11×10^{-5}, thus qualifying as hydraulically smooth. It was mounted on a sting of diameter 6 mm ($=d/6.3$). In both cases, the sting is slender enough to avoid problems associated with sting/wake interactions.

Each sting could be attached to a vertical strain-gauged cantilever, as shown in Fig 2(a), the gauges forming one arm of a Wheatstone bridge network. Calibration was by static load and the out-of-balance voltage was fed to a time-averaging digital voltmeter. A metal wedge-shaped guard was placed in front of the vertical arm and attached to a traversing mechanism. This prevented the strain gauges measuring anything other than the hydrodynamic force on the sphere. The traversing mechanism enabled the spheres to be moved along all three axes, up to a maximum distance downstream x of 2.6 m, x being measured from the upstream extremity of each grid. All drag testing was carried out on the flow centreline; the ability to move in the y and z directions merely enabled the sphere to be positioned on that centreline.

Air speed in the region of the sphere was measured using a standard pitot-static tube, attached to an electronic micromanometer. A constant temperature hot-wire anemometer (CTA) was also mounted nearby for measuring turbulence intensity. These two probes were mounted vertically above the sphere stagnation point and careful manoeuvering showed that the presence of a sphere had little effect on probe readings, if they were

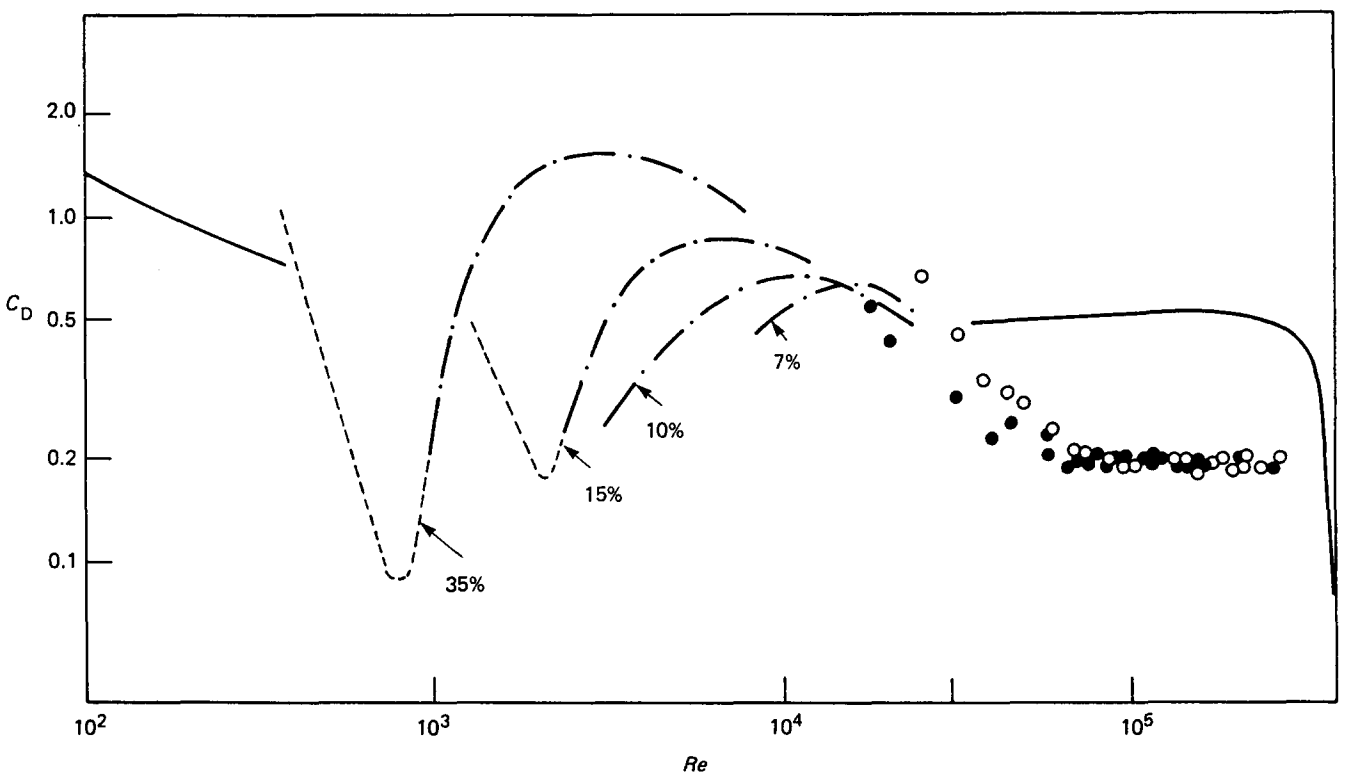

Fig 1 The effect of high turbulence intensities on drag coefficients—a comparison of previous results. ○ I = *10%*, ● I = *15%*, *Neve*[3]; — *Achenbach*[6]; ------ *Torobin and Gauvin*[5]; -·-·- *Clamen and Gauvin*[7]

Notation

b	Grid slat width
C_D	Drag coefficient based on frontal area
d	Sphere diameter
I	Relative turbulence intensity ($=u'_{rms}/\bar{u}$)
k	Relative sand roughness (Nikuradse)
L_x	Longitudinal turbulence macroscale
L_y	Lateral turbulence macroscale
M	Grid mesh (distance between slat centrelines)
Re	Reynolds number ($=\bar{u}d/\nu$)
u'_{rms}	Streamwise velocity rms fluctuating component
$\bar{u}$	Streamwise velocity (time mean value)
x	Axial distance from grid
y	Horizontal distance of sphere from jet centreline
z	Vertical distance of sphere from jet centreline
ν	Kinematic viscosity of air

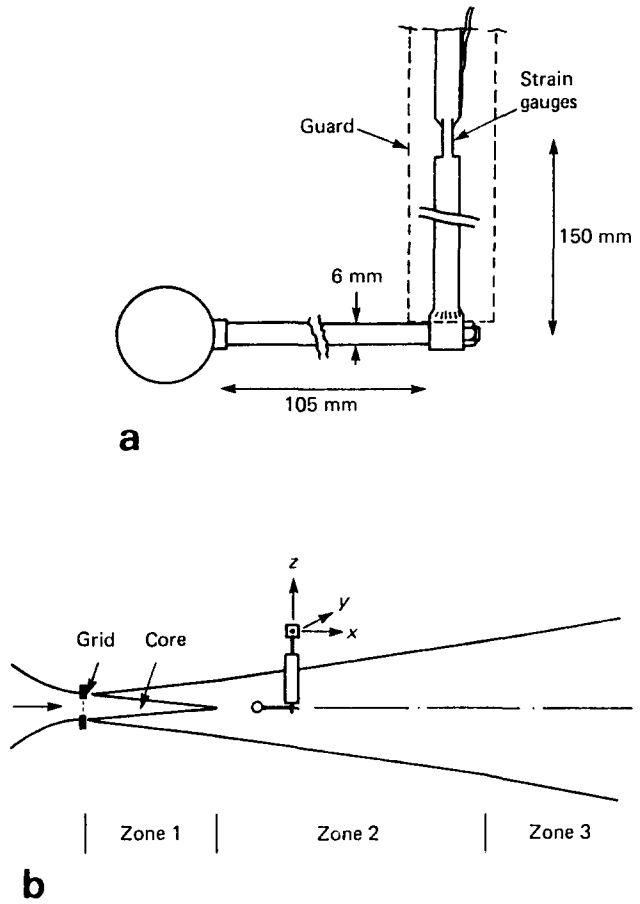

Fig 2 Experimental arrangement. (a) Strain-gauged force transducer. (b) Wind tunnel exit and jet zones

mounted at least three sphere radii above the centreline. For testing, the hot wire was therefore mounted at a height of 3 radii above and the pitot tube at 3.8 radii. Even though one has no alternative to this, since the probes clearly cannot be mounted at exactly the same point as the sphere, some justification is needed here for not applying position corrections, which is explained in the following text.

In the absence of a grid at the tunnel exit plane, a jet will be formed as shown in Fig 2(b) with three clearly different zones. Zone 1 is characterized by an 'inviscid core' surrounded by a region where shearing stresses are high because of the action of the jet edge on the surrounding atmosphere. In Zone 2, the mixing regions from both sides have reached the centreline and further mixing takes place before Zone 3, where the jet has become 'self-preserving' with mathematically similar velocity profiles. The start of Zones 2 and 3 are normally at about 5 and 20 nozzle widths downstream, although the latter figure can sometimes be as high as 30 (Ref 8).

In the presence of a grid, Zone 1 is modified in the sense that it now represents the total of many small inviscid cores, each caused by one grid hole. A probe on the centreline of Zone 1 would no longer therefore measure a very low turbulence constant air speed but would give results dependent upon its axial station x M. Taylor[9] has reported that for grid bars as broad as $b = M$ 4, the 'shadow' of the grid disappears after a few mesh widths downstream but that for grids with a very low b M value, the shadow can last up to at least $x = 20M$.

In this present work, some preliminary testing showed that for Grid A ($b/M = 0.278$) and probes positioned at $x = 480$ mm ($x/M = 5.33$), the velocity on a slat centreline was only 94% of that on a hole centreline and the turbulence intensity varied laterally between a low of 15.9% and a high of 18.3% at the same station downstream.

These figures seem to justify Taylor's comments and also Dryden's fear of losing homogeneity of turbulence if x/M became too small. They also point to the probability that testing in the core region of Zone 1 is justified provided that the sphere and probes are all inside the core in the lateral sense and at least seven or eight mesh widths downstream of the grid. Turbulence intensities should then vary laterally by no more than a couple of percentage points, allowing the probes to be mounted at up to 3.8 sphere radii off the centreline without corrections being needed. In Zones 2 and 3, the lateral separation of probes and sphere would represent such a tiny proportion of jet width that no correction is thought necessary here either. The main requirement is clearly to avoid regions of high shear and testing on the jet centreline only should ensure this.

These various criteria were obviously much easier to satisfy with the small sphere than with the large one so the latter was used in only a limited number of cases where a larger value of d was required for minimizing the ratio of turbulence scale to sphere diameter or for maximizing Reynolds number. These few cases are described in more detail later.

The hot-wire anemometer was used to measure both the relative turbulence intensity and the longitudinal scale L_x. A linearizer was inserted in the CTA circuit since all testing would be undertaken at turbulence intensities comfortably above the figure of a few percent normally used as a criterion for linearizer inclusion. Turbulence macroscale downstream of the grids was measured in the absence of spheres using the same CTA hot wire and rms voltmeter connected to a Brüel and Kjaer tunable bandpass filter. A power spectral density (PSD) technique was then employed to assess scale. Two slightly different versions of this technique were available. One involves plotting spectral density (energy in waveband divided by bandwidth) against frequency and extrapolating to zero frequency to determine a parameter proportional to L_x. The other involves plotting the product of spectral density and frequency against frequency and determining a value of the latter at which a peak occurs. A standard curve for this second approach is given in E.S.D.U. Data Sheet 74031 (Aerodynamics, Vol. 6) and L_x is then obtained from the reciprocal of that frequency.

The latter method is not always easily applicable because the peak is sometimes ill-defined so the former method has been used here. Even then, this was considered to be the most convenient rather than the most accurate method for scale determination. However, it was satisfactory for this application since an approximate measure of L_x is sufficient for assessing the effects of L_x d; it will be seen subsequently that results scatter does not warrant a more rigorous approach.

Experimental testing was based on the idea of varying Reynolds number by adjusting wind tunnel airspeed and accepting whatever values of I and I_x obtained at the chosen downstream position x. The sphere would then be moved to a different location, with

different I and L_x, and the process would be repeated. Various combinations of I and L_x could be obtained using different grids but the region upstream of about seven mesh widths for each grid was avoided. Different values of L_x/d and Re could also be obtained by changing sphere but the vast majority of tests were carried out with the smaller sphere because the low Reynolds number end of the spectrum was generally of more interest in the present context.

If a data point is represented by combined values of Re, C_D, I and x, then 626 such points were obtained over several months of testing and stored on floppy disk. Turbulence scale was taken for each point from Fig 3, obtained during the PSD testing mentioned above, and also stored at the appropriate location on the disk so that analysis could then be undertaken by plotting C_D versus Re for given I and L_x/d values, within specified bandwidths.

Accuracy

This project was concerned with measuring drag forces under a variety of different flow conditions and the accuracy of measuring each parameter was not uniform. The use of time-averaging digital meters in all cases except the rms voltmeter for turbulence intensity led to reasonably stable values being obtained with integrator time constants of typically 3 seconds. The least accurate results obtained were for turbulence scale, because of the PSD technique used, and for C_D values at the lowest Reynolds numbers. The accuracy of the former is indicated by the limit bars in Fig 3 and is not considered critical since even a 15% error in L_x/d still gives a good idea of scale. Errors in C_D are more serious and values at the lowest Reynolds numbers should be used only for assessing trends. At these low speeds, forces typically represented by 20 mV on the voltmeter were liable to vary between 18 and 22 mV. At the other extreme, of high airspeeds, there was no difficulty in measuring forces represented by 1450 mV. The calibration factor for the force balance was 0.4787 N/Volt.

Experimental results

Turbulence scale and intensity

It is instructive to compare the results obtained here with other published values. In Zone 1 the hot wire probe senses a flow which has recently passed through a grid whereas in Zone 3 it is in the developing or developed region of a large jet having a very turbulent core region. In the former case one would expect the results to be similar to those of Baines and Peterson[10] and of Bearman[11] for flows downstream of grids whereas in the latter case one would expect reasonable agreement with a whole host of published results for turbulence in jets, wakes and mixing layers.

Considering macroscale first, Fig 3 shows results obtained with all three grids. In each case, there is clearly a transition from a lesser rate of increase of L_x with x in the vicinity of the grids to a steeper value in the developing jet region. Superimposed line 1 corresponds to Bearman's results and line 2 to those of Baines and Peterson. A slight complication here is that Baines gave results only for L_y so these have been multiplied by 2.7, this being the ratio of L_x:L_y found by Wygnanski and Fiedler[12] for the turbulence on the higher velocity side of a mixing layer. The present results agree well with these two lines, where the measuring position was close enough to the grid to be in the wind tunnel jet core. Downstream, the results rise above the lines, eventually corresponding to scale being proportional to distance from the wind tunnel exit plane. The constant of proportionality varies somewhat in other published work from about 0.09 in the case of Townsend[13] dealing with plane wakes, to about 0.13 in the case of Davies *et al*[14] who dealt with circular jets. The bulk of published figures are close to the value of 0.098 given by Wygnanski and Fiedler[12] and the present results are seen in Fig 3 to fit roughly between lines 3 and 4 representing respectively, $L_x = 0.07x$ and $0.10x$.

The data points shown in this figure represent the extreme values of L_x obtained at the indicated x/b values; accuracy is considered adequate in view of the method used and greater accuracy is not in any case required here.

In the case of turbulence intensity, Fig 4 shows the results for all three grids versus downstream location on the centreline. Once again, a transition is evident in all cases from a state of relative intensity decreasing with downstream motion to a minimum point followed by a fairly rapid climb towards the value of about 23% normally associated with jet centrelines. Vertical bars indicate the range of values of I obtained at a given x/b value and it is generally true to say that highest values of any bar correspond to lowest Reynolds number and vice versa. The fact that results have been obtained close to grids is no guarantee of isotropy and drag results given later for spheres subjected to turbulence intensities greater than about 15% were generally obtained from stations giving high x/b values rather than low ones. Lines have been superimposed to represent the data of Baines and Peterson[10] and Taylor[15] and agreement for 'core region' results is seen to be fairly good.

Low intensity and small scale

The known effects of turbulence of very small scale and fairly low intensity are evident in Fig 5. As a check on drag

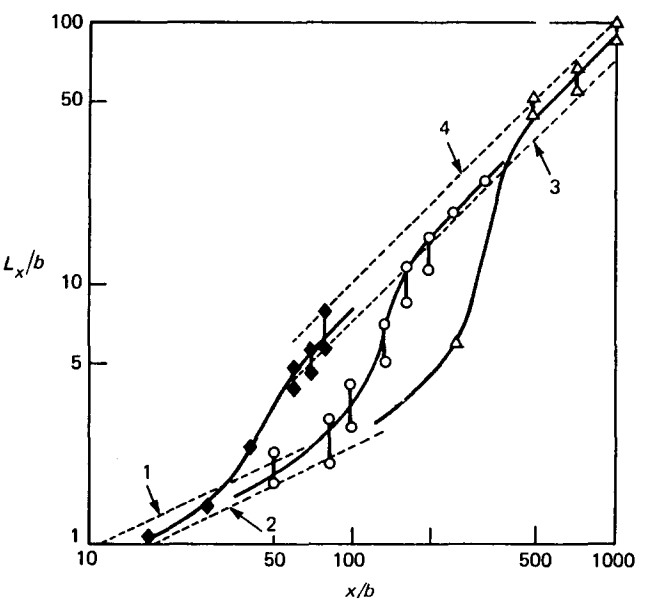

Fig 3 Turbulence macroscale downstream of the grids (centreline values). ◆ *Grid A;* ○ *Grid B;* △ *Grid C. Line 1, results of Bearman*[11]*; line 2, Baines and Peterson*[10]*; line 3,* $L_x = 0.07x$*; line 4,* $L_x = 0.10x$

force transducer accuracy, the small sphere was mounted in the Zone 1 core with no grid attached to the wind tunnel. The C_D values are seen to follow Achenbach's classical curve[6] very closely. As a further check the large sphere was used with the finest grid to obtain C_D values at very low L_x/d levels, but with turbulence intensity of a few percent. These tests are open to objection on the grounds that the large sphere represents a 10.7% blockage for the tunnel exit plane and therefore unrepresentative C_D values could be obtained. The small sphere constitutes a blockage of only just over 1%. Even so, the data points on Fig 5 clearly show the same trend of decreasing critical Reynolds number with increasing turbulence intensity as was found by Dryden[4]. These results rise above the standard curve at lower Reynolds numbers and superimposition of Clamen and Gauvin's curve[7] for 7% shows that they also encountered a higher subcritical drag coefficient. Comparison with the present author's previous results[3] is not possible because no attempt was made on that occasion to measure scale but the trend is the same.

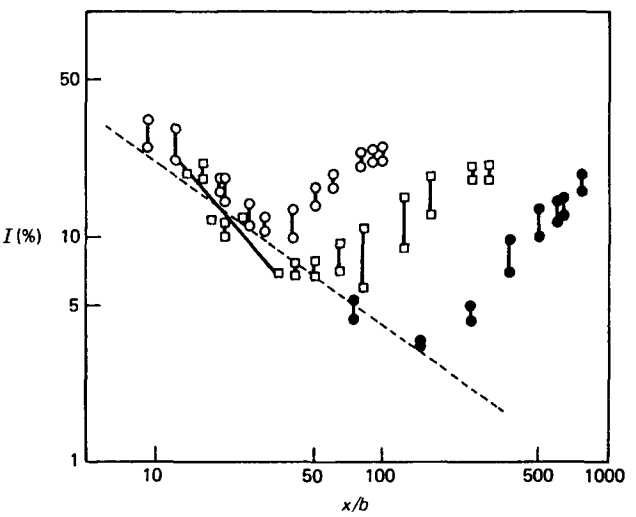

Fig 4 Turbulence intensity downstream of the grids. (centreline values.) ○ *Grid A;* □ *Grid B;* ● *Grid C.* ----- *Baines and Peterson*[10], —— *Taylor*[15] *apply to region 1 'core' only*

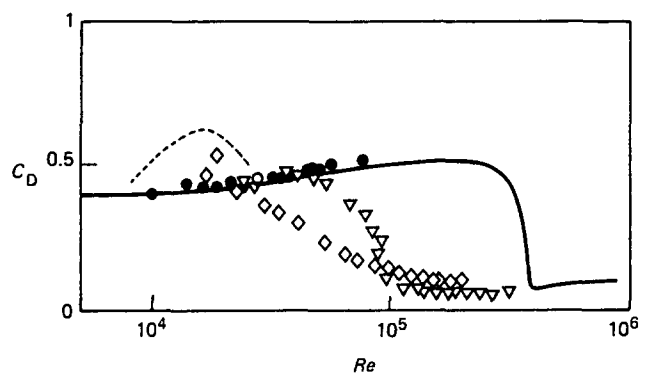

Fig 5 Drag coefficient for small scale and low intensity turbulence. ● I = *0.4%*, $L_x/d = 0$; ▽ *4%, 0.06*; ◇ *7%, 0.08*; —— *Achenbach*[6]; ------ *Clamen and Gauvin*[7], I = *7%*

Intermediate and high intensity results

Results for drag coefficient versus Reynolds number for various bands of turbulence intensity and approximate L_x/d values are given in Figs 6, 7 and 8. In all three of these figures the graph (a) on the left shows the data points actually obtained but it is easier to recognize and discuss trends by reference to the simplified drawing (b) on the right in each case. A lengthy description of these graphical results would be tedious and a possible interpretation of them is contained in the next section so here it must suffice to deal with general trends, where they can be spotted.

With turbulence intensities of around 10%, Fig 6 conforms to the usual tendency for critical Reynolds number to be lowered as I is increased. As turbulence scale is increased at this same value of I, the critical Reynolds number is lowered still further but at L_x/d greater than unity there is an interesting new development in that supercritical C_D values rise again to levels more typical of subcritical Reynolds numbers, producing an S-bend appearance in the drag curves.

As turbulence intensity is increased, the same trends are evident (Figs 7 and 8) with the additional factor that as I becomes higher the characteristic rightwards fall of the C_D curves at higher Reynolds numbers is maintained to greater L_x/d values before the onset of any S-bend tendencies. At the highest intensities of all (Fig 8),

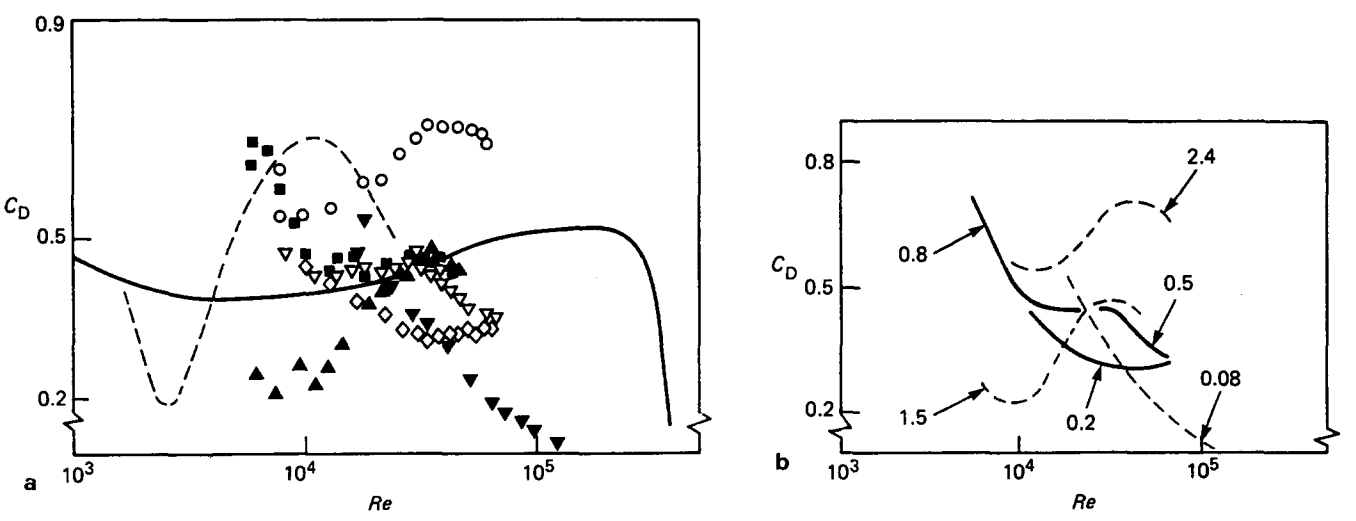

Fig 6 The effect of turbulence scale on drag coefficient; I = *10% ± 2%,* L_x/d *values shown: (a)* ▼ *0.08;* ◇ *0.2;* ▽ *0.5;* ■ *0.8;* ▲ *1.5;* ○ *2.4.* —— *Achenbach*[6]; --- *Clamen and Gauvin*[7], I = *11%; (b) simplified plot of results from this work shown in (a)*

and L_x/d value of 3 produces the highest C_D whereas values of 3.8 and 4.2 indicate an apparent return towards standard curve values.

The superimposition on these figures of lines representing the results of Clamen and Gauvin[7] show that they too were obtaining S-bend curves, even if their peaks and troughs occurred at different Reynolds numbers from the current results, so some profound changes in flow conditions near the sphere are suggested by the combined data.

A final point of interest from Figs 7 and 8 is that with the correct combination of turbulence intensity and scale, C_D can vary markedly at constant Reynolds number. These areas are shown shaded in Figs 7(b) and 8(b) and it should be noted that the results therein were repeatable.

Discussion of results

Some basic considerations

Graphical results described in the previous section clearly indicate some turbulence scale effects but a more detailed assessment of what the effects result from is possibly best achieved by following a few general guidelines based on existing knowledge. There can be little doubt, for example, that we are looking at the results of marked changes in pressure rather than in skin friction. Achenbach[6] has shown that even across the fundamental changes in flow conditions induced by boundary layer transition at the critical condition, skin friction contribution to total drag increases from only about 1.2% to about 13%.

Changes in C_D are therefore likely to be induced by two principal causes. Free stream turbulence is known to have a strong influence on boundary layer state and therefore on separation position around the sphere. Turbulence scale and intensity are thought to influence wake conditions strongly because of the considerable mixing of wake and free stream which is likely to occur at high values of I and L_x. A high value of intensity could therefore produce a low C_D because a turbulent boundary layer would separate later from the sphere, causing a narrower wake. On the other hand, high turbulence in the

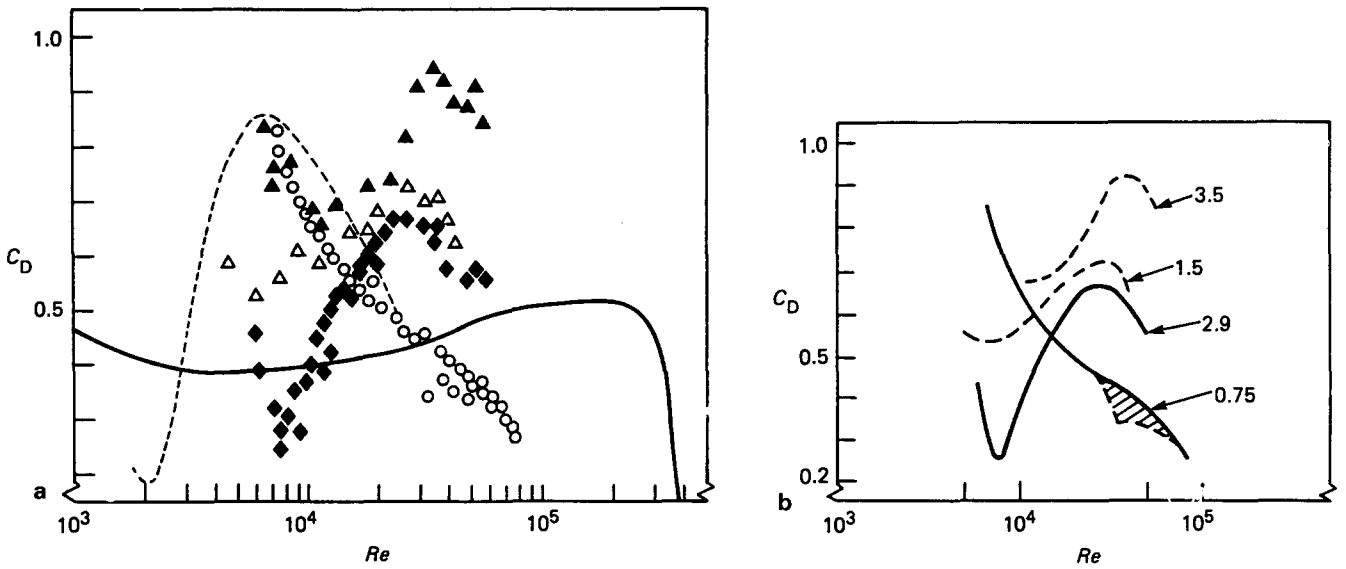

Fig 7 The effect of turbulence scale on drag coefficient: I = 16% ± 2%. L_x/d *values shown:* (*a*) ○ *0.75;* △ *1.5;* ◆ *2.9;* ▲ *3.5;* — *Achenbach*[6]*;* --- *Clamen and Gauvin*[7], I = 15%*;* (*b*) *simplified plot of results from this work shown in* (*a*)

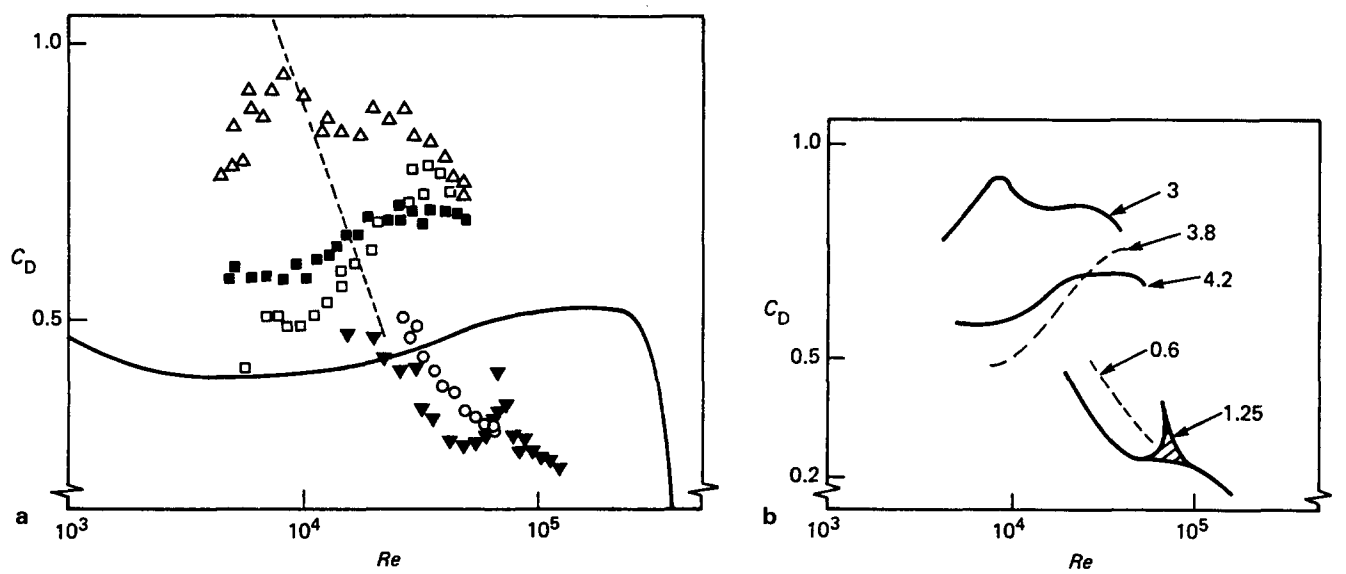

Fig 8 The effect of turbulence scale on drag coefficient; I = 22% ± 2%. L_x/d *values shown:* (*a*) ○ *0.6;* ▼ *1.25;* △ *3;* □ *3.8;* ■ *4.2.* — *Achenbach*[6]*;* --- *Clamen and Gauvin*[7], I = 23%*;* (*b*) *simplified plot of results from this work shown in* (*a*)

free stream can also cause increased mixing with the wake and therefore a higher C_D value because of the lower base pressure thereby induced. The flow close to the sphere could therefore reflect elements of both these influences and the supervening battle will determine the level of drag coefficient actually obtained. It may be that a stable result is not obtained, in which case the value of C_D could oscillate between quite wide limits. This type of instability is perhaps evident in the $L_x/d=0.75$ and 1.25 curves of Figs 7 and 8, already alluded to.

As an extreme case, when L_x/d becomes very large, the sphere will simply 'see' a periodically varying laminar flow of alternating positive and negative incidence and C_D might then revert to its standard curve levels.

Effects on drag coefficient

If the assumptions made above are reasonable, then some interpretation can be attempted of the trends in C_D described in the previous section. The graphs of Figs 6, 7 and 8 show similar effects, so Fig 6 will be dealt with as typical of them all.

At the relatively high Reynolds number of 50×10^3, turbulence of $I=10\%$ and $L_x/d=0.08$ has produced a low drag coefficient indicating premature transition of the sphere boundary layer and a narrow wake. As scale is increased to $L_x/d=0.2$, 0.5 and eventually to 1.5, C_D is seen to increase, presumably indicating a widening of the wake resulting from increased mixing with the turbulent free stream. At $L_x/d=2.4$ this process has led to a value of C_D well above the standard curve value for $Re=50\times10^3$.

At Reynolds numbers slightly less than 10×10^3 another interesting change has occurred. For scales up to $L_x/d=0.8$, C_D has a value not much different from the standard curve, indicating presumably a laminar boundary layer and wide wake. As Reynolds number falls, the C_D value climbs, indicating an even wider wake resulting from mixing with the free stream. This is even the case for $L_x/d=2.4$ but at a scale of 1.5 a severe, repeatable, drop in C_D occurs, to levels associated with turbulent boundary layers. Clearly this combination of scale and intensity has produced a profound change in flow conditions, resulting in the drag curve taking on a pronounced S-bend appearance similar to those of Clamen and Gauvin[7]. The fact that the present results reproduce the general shape of Clamen and Gauvin's but at different Reynolds numbers must indicate the possibility that some other agency is also affecting C_D. Their results were obtained exclusively in pipe flows with quoted scale values L_x/d between about 2 and 6 whereas the results reported here were obtained in what was effectively a very large jet flow so the possibility must be faced that, for example, the turbulence spectrum is also an important factor.

At higher turbulence intensities (Figs 7 and 8) the overall trends are the same with the marked changes occurring at higher L_x/d values as I is increased. This suggests the possibility that scale and intensity generally have opposing effects on C_D. In addition, Fig 8 shows that the value of $L_x/d=4.2$ is just high enough to produce a trend back towards standard curve values, as suggested before.

The combined effects of scale and intensity are probably better seen if appropriate results are cross-plotted in terms of spot values of drag coefficient (or C_D values within specified narrow ranges) plotted on a graph having axes of L_x/d and I, all at a specified Reynolds number. For the interesting region $7000\leqslant Re\leqslant8000$, this type of plot is shown in Fig 9. Although the C_D 'contour lines' may be rather vague, there is clearly an identifiable region, running almost diagonally, where the combination of L_x/d and I results in markedly lower drag coefficients. Moreover, the change from values of C_D around 0.6 or 0.7 just outside the region to values around 0.2 just inside it suggests that the process involved is a sudden one, akin to boundary layer transition.

If the same plotting technique is applied to results around $Re=50\times10^3$ the graph of Fig 10 is obtained. The form of this is rather more predictable in the sense that passing from low to high values of L_x/d at constant intensity causes C_D to increase more gradually from low to high values, with a single point indication at high I and high L_x/d that C_D is just starting to return to the standard curve (laminar) value of 0.48.

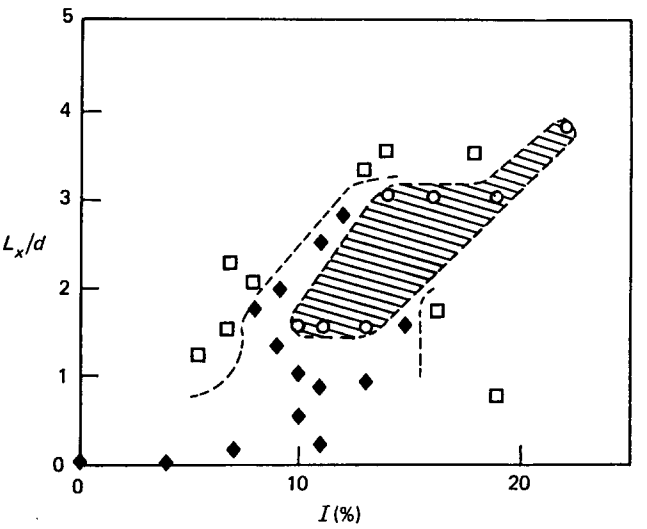

Fig 9 Combined effects of scale and intensity on drag coefficient: $7000\leqslant Re\leqslant8000$. C_D ranges shown: ○ <0.4; ◆ 0.4 to 0.6; □ >0.6. Shaded area is low-drag zone

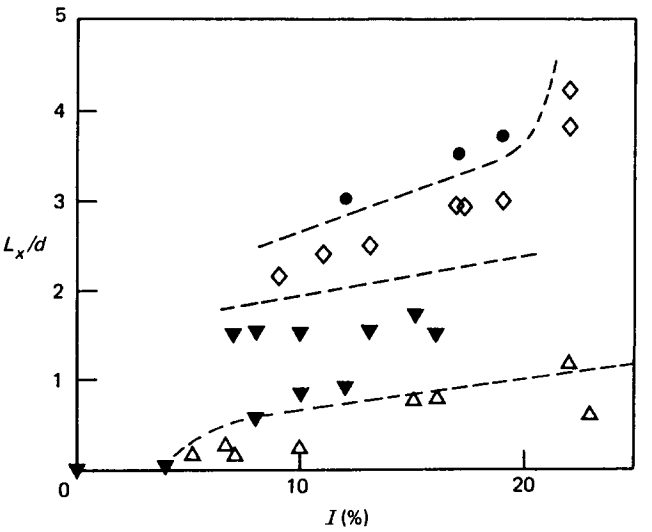

Fig 10 Combined effects of scale and intensity on drag coefficient: $Re=50\times10^3$. C_D ranges shown: △ <0.4; ▼ 0.4 to 0.6; ◇ 0.61 to 0.89; ● ≥0.9

Comparison with heat transfer results

The overall impression given so far by these results is that scale and intensity are both important in determining the level of drag coefficient for spheres and that certain combinations of these two parameters can cause sudden and profound changes in the flow adjoining them. Various authors have experimented with the heat transfer from spheres in turbulent flows and, although they have obviously been concerned with Nusselt numbers rather than drag coefficient, their results shed light on the current problem.

In dealing with cylinders, Van der Hegge Zijnen[16] suggested that a resonance condition might be obtained when the frequency of the energy-containing eddies in the free stream was half the vortex shedding frequency of the cylinder itself. Strictly speaking, this is not necessarily applicable to spheres but the latter do have a characteristic shedding frequency of their own so similar conditions might apply. For Van der Hegge Zijnen, Nusselt number reached a peak at about $L_x/d=1.6$ for $I=12\%$ and $Re=9550$, this peak being about 60% higher than for $L_x/d=0$. The following year, Hinze[17] showed analytically that a resonance ought to occur at about $L_x/d=1.2$, which is fairly close to Van der Hegge Zijnen's experimental value.

Galloway and Sage[18], Raithby and Eckert[19], Raithby[20] and Mujumder and Douglas[21] have all tested spheres in turbulent flows but have failed to find a heat transfer resonance condition similar to Van der Hegge Zijnen's. Indeed, Raithby has implied that Van der Hegge Zijnen's results are unique even for cylinders. However, Mujumder and Douglas, for example, quote turbulence limits ($I=12.6\%$, $L_x/d=1.34$) which put them just below the sensitive low C_D area in Fig 9, their Reynolds numbers being comparable. It could be therefore that a slight increase in scale might have triggered a marked change in flow conditions to give a different Nusselt number. Van der Hegge Zijnen's results may therefore be unique simply because no other experimenter has since entered the correct zone of scale and turbulence to reproduce Van der Hegge Zijnen's effects. Future tests may yet produce changes in heat transfer coefficient comparable with the marked C_D changes encountered in this present work.

Conclusions

This project set out to determine whether turbulence macroscale was an important factor in determining sphere drag coefficient; the results suggest that it is. Even allowing for known experimental inaccuracies, both the trends and the important quantitative results are repeatable. When L_x/d is low, C_D values are obtained which are comparable with other, though rather limited, published values. At the other extreme, when L_x/d has a value greater than about 4, the results suggest that C_D is starting to return to standard curve values, having been well above these when scale and diameter were comparable. In the region $0.5<L_x/d<3$, however, a very involved relationship seems to exist between drag coefficient and scale which tends to be in accordance with the conclusions reached by Van der Hegge Zijnen experimenting with heat transfer rates from cylinders, the obvious assumption here being that the same marked changes in flow conditions which produce a change in C_D also affect the overall heat transfer coefficient.

More importantly, though, in certain Reynolds number ranges the correct combination of Re, I and L_x/d can produce sudden repeatable changes in C_D of a magnitude suggesting a profound change in flow conditions at the sphere surface and in the wake. A clearer understanding of the flow processes involved here would require additional instrumentation since the condition of the boundary layers and wake and also the positions of separation and transition points would all need to be monitored at the same time. This therefore represents the next stage in gaining a better understanding of the importance of macroscale.

Acknowledgements

This project was funded entirely from UGC sources and the author wishes to express his gratitude to the Department of Mechanical Engineering at The City University for the facilities provided. Thanks are also extended to Mr D. M. Sykes of the Department of Aeronautics, both for the loan of equipment for measuring turbulence scale and also for his helpful comments during the prosecution of this project.

References

1. **Neve R. S. and Kotsiopoulos P.** Drag coefficient corrections for spheres in thin circular jets. *The Aeronautical Journal, 1980*, **84**, *386–387*
2. **Neve R. S., Kotsiopoulos P. and Nelson R.** The drag force on spheres in thin jets. *J. Fluid Mech., 1981*, **107**, *521–531*
3. **Neve R. S. and Jaafar F. B.** The effect of turbulence and surface roughness on the drag of spheres in thin jets. *The Aeronautical Journal, 1982*, **86**, *331–336*
4. **Dryden H. L. et al.** Measurements of intensity and scale of wind tunnel turbulence and their relation to the critical Reynolds number of spheres. N.A.C.A. Tech. Rep. 581, *1937*
5. **Torobin L. B. and Gauvin W. H.** The drag coefficients of single spheres moving in steady and accelerated motion in a turbulent field. *J.A.I.Chem.E., 1961*, **7**, (*4*), *615–619*
6. **Achenbach E.** Experiments on flow past spheres at very high Reynolds numbers. *J. Fluid Mech., 1972*, **54**(*3*), *565–575*
7. **Clamen A. and Gauvin W. H.** Effects of turbulence on the drag coefficients of spheres in a supercritical flow regime. *J.A.I.Chem.E., 1969*, **15**(*2*), *184–189*
8. **Wygnanski I. and Fiedler H.** Some measurements in the self-preserving jet. *J. Fluid Mech., 1969*, **38**(*3*), *577–612*
9. **Taylor G. I.** *The statistical theory of turbulence—Part I, Proc. Roy. Soc., 1935*, **A151**, *421–444*
10. **Baines W. D. and Peterson E. G.** An investigation of flow through screens. *Trans. ASME, 1951*, **73**, *467–480*
11. **Bearman P. W.** An investigation of the forces on flat plates normal to a turbulent flow. *J. Fluid Mech., 1971*, **46**, *177–198*
12. **Wygnanski I. and Fiedler H.** The two-dimensional mixing region. *J. Fluid Mech., 1970*, **41**(*2*), *327–361*
13. **Townsend A. A.** The structure of turbulent shear flow. *Cambridge University Press, 1956*
14. **Davies P. O. A. L. et al.** The characteristics of the turbulence in the mixing region of a round jet. *J. Fluid Mech., 1963*, **15**, *337–367*
15. **Taylor G. I.** *The statistical theory of turbulence—Part II, Proc. Roy. Soc., 1935*, **A151**, *444–454*
16. **Van Der Hegge Zijnen B. G.** Heat transfer from horizontal cylinders to a turbulent air flow. *Appl. Sci. Res., 1958*, **A7**, *205–219*
17. **Hinze J. O.** *Turbulence, McGraw-Hill, N.Y., 1959, 558–560*

18. **Galloway T. R. and Sage B. H.** Thermal and material transfer from spheres. Prediction of local transport. *Int. J. Heat and Mass Transfer, 1968*, **11**, *539–549*

19. **Raithby G. D. and Eckert E. R. G.** The effect of turbulence parameters and support position on the heat transfer from spheres. *Int. J. Heat and Mass Transfer, 1968*, **11**, *1233–1252*

20. **Raithby G. D.** Comments on eddy shedding from a sphere in turbulent free streams. *Int. J. Heat and Mass Transfer, 1971*, **14**, *1875*

21. **Mujunder A. S. and Douglas W. J. M.** Eddy shedding from a sphere in turbulent free streams. *Int. J. Heat and Mass Transfer, 1970*, **13**, *1627–1629*

BOOK REVIEW

Measurement Techniques in Heat and Mass Transfer

Ed. R. I. Soloukhin and N. H. Afgan

This recent book provides a mass of practical information and guidelines for those involved in evaluating, planning or implementing cogeneration (combined heat and power) projects in industrial, commercial and domestic situations.

The fourteen chapters cover a range of topics, including feasibility assessment, analytical methods for technical and economic feasibility evaluation, computerized system design, cogeneration technologies and application considerations, plus non-conventional technologies (such as waste heat recovery and the use of refuse derived fuel).

Readers will find that the book has been written with the United States regulatory environment in mind.

Cogeneration represents a classic case of how changing economic conditions can give an old technology new life. It has been practised since the turn of the century, but had declined steadily in importance in the USA for several decades. However, the events of the 1970s placed energy efficiency in a new, favourable light and led to a great resurgence of interest. This interest can be appreciated when we read that nearly half the primary energy consumed by US industry and electricity producers is lost as waste heat, totalling over seven million barrels per day of oil equivalent.

Throughout the text there are frequent references to the Public Utility Regulatory Policies Act (PURPA) and the National Energy Act of 1978 which removed many of the institutional and financial barriers to cogeneration. These Acts and other legislation appear to have opened the door to numerous cooperative ventures between industry and local electricity utilities.

One paper examines the potential for fuel cell-based cogeneration. This will continue a growing trend in small-scale prepackaged cogeneration systems.

Reducing the size at which cogeneration becomes economic will mean that these systems will exponentially expand the number of potential sites. Prospective new consumers will include anyone with a demand for both power and heat, such as hospitals, educational establishments, shopping centres, high-density housing developments and small industry. One author thought that more than 10,000 MW of new small cogeneration capacity could be installed in the next decade. These new small-scale, independent electricity producers could have a profound effect on the electricity industry of the USA and ultimately other countries.

Cogeneration will almost certainly continue to increase in importance in the coming years because of both the economic arguments (mainly the high cost of electricity) and the energy conservation potential.

Despite the fact that this book was produced for the USA market (with appropriate examples and non-SI units) it should prove to be of great value to those who are interested in this important field.

Tze Yao Chu
Geothermal Research Division,
Sandia National Laboratoratories,
USA

Published, price $84.50, by Hemisphere Publishing Corporation, 79 Madison Ave, New York, NY 10016, USA, 569 pp.